

E-9-1 (Invited)

Distributed Feedback and Mode Locked Silicon Evanescent Lasers

Alexander W. Fang, Brian R. Koch, Erica Lively, Daniel J. Blumenthal, John E. Bowers

University of California Santa Barbara, ECE Department
 Santa Barbara, CA 93106-9560, USA
 Phone: +1-805-893-4883, E-mail: awfang@ece.ucsb.edu
 (Invited)

1. Introduction

New integrated photonic integrated circuit (PIC) platforms that combine the best of silicon and III-V (InP) properties have matured to the point where complex laser structures can be fabricated. In this article we describe recent progress on Distributed Feedback (DFB) and Mode Locked (ML) silicon evanescent lasers and report on the laser design and performance. We also describe recent developments in silicon evanescent lasers that utilize surface corrugated gratings in the silicon waveguide to create distributed feedback lasers [1] and racetrack resonator topographies in conjunction with saturable absorbers to create mode-locked racetrack lasers [2].

2. Silicon Evanescent PIC Platform

The silicon evanescent PIC platform consists of thin crystalline III-V films transferred to silicon waveguides. This platform utilizes silicon waveguide processing in order to define the device topography and cavity while still achieving electrically pumped gain, modulation, and detection from the III-V regions and has resulted in the demonstration of lasers, amplifiers, detectors, and modulators [3-5].

3. Distributed Feedback Silicon Evanescent Lasers

Distributed feedback lasers are attractive for WDM applications since they have a single longitudinal mode output and their short cavity lengths allow for low threshold currents while still producing output powers in the mW regime. Figure 1 shows a diagram and SEM of the longitudinal cross section of a distributed feedback silicon evanescent laser (DFB-SEL). A ~25 nm surface corrugated grating with a 238 nm pitch and 71 % duty cycle surface corrugation is formed on the silicon waveguide prior to wafer bonding. The grating κ , $\sim 247 \text{ cm}^{-1}$, is large due to the high index of the III-V layers, resulting in higher grating-modal overlap than oxide clad surface corrugated gratings in silicon. The grating is 340 microns long with a quarter wavelength shift (QWS) in the center, resulting in a κL of 8.4.

The L-I-V curve is shown in Figure 2, with a device lasing threshold of 25 mA and maximum output power of 5.4 mW, at 10°C. This corresponds to a threshold current density of 1.4 KA/cm^2 , which is slightly lower than the 2 kA/cm^2 and 1.7 KA/cm^2 seen in previously demonstrated Fabry-Perot and

Racetrack SELs, respectively [1]. The maximum lasing temperature is 50 °C.

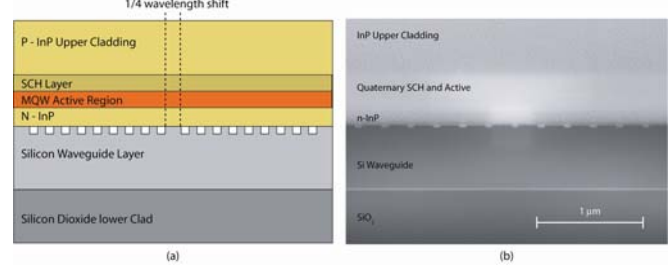


Figure 1: a) DFB-SEL cross sectional diagram and b) SEM.

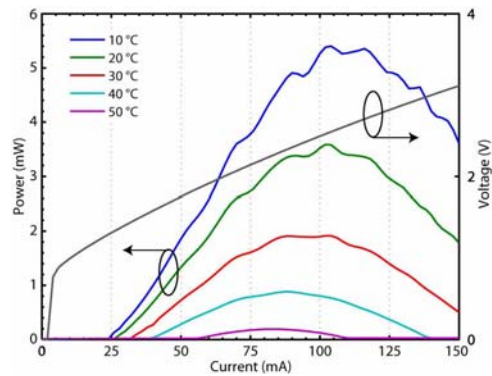


Figure 2: L-I-V curve of the DFB-SEL versus temperature.

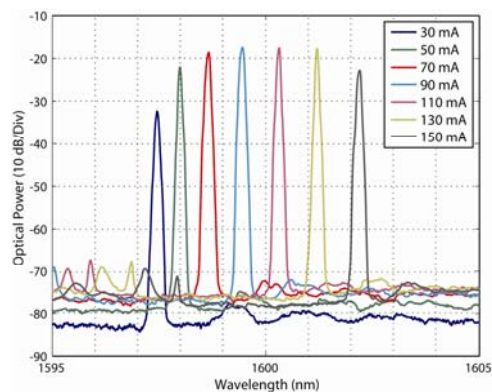


Figure 3: Continuous wave lasing spectrum for various current levels.

Figure 3 shows the spectral shift under CW operation for various current levels. It can be seen that the laser stays single mode throughout the various current injection levels. The change in wavelength versus electrical dissipated power ($d\lambda/dP$) and wavelength versus stage temperature under pulsed operation ($d\lambda/dT$) is 12.849 nm/W and $0.0971 \text{ nm/}^\circ\text{C}$,

respectively. The resulting thermal impedance is 132 °C/W. This value is higher than the 40 °C/W measured on 850 micron long Fabry-Perot SELs but scales appropriately due to the DFB-SEL's short device length. The laser line width is measured at 3.6 MHz by using the delayed-self heterodyne method.

4. Mode-locked silicon evanescent lasers

Mode-locked lasers (MLLs) are capable of generating stable short pulses which have a corresponding wide optical spectrum of phase correlated modes. MLLs can have high extinction ratios, low jitter, and low chirp, making them excellent transmitters when combined with a data-encoding modulator. Figure 4 shows an SEM of a racetrack mode-locked laser with a 2.657 mm long racetrack resonator and a 30 μm long saturable absorber. The gain section is driven at 410 mA while the saturable absorber is DC biased with -0.66 volts. Mode-locking occurs via colliding pulse mode-locking (CPM) with clockwise and counter clockwise pulses colliding simultaneously in the saturable absorber at a rate ~30 GHz as determined by the cavity length and group index of refraction. The device is temperature stabilized on a stage held at 10 °C.

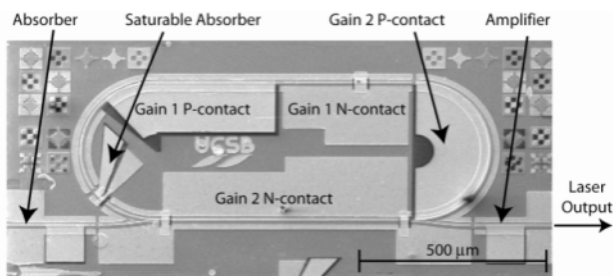


Figure 4: SEM of the racetrack mode-locked silicon evanescent laser.

When all sections (gain and the saturable absorber) are connected and forward biased together in parallel, the laser threshold was measured to be 250 mA. The autocorrelator pulse traces for passive mode-locking and hybrid mode-locking are shown in Figure 5. The autocorrelated pulse width was measured at 10 ps. A 7 ps pulse width is estimated by assuming a Gaussian pulse shape. The average power of the counter-clockwise pulses is measured at 1.92 mW. This corresponds to a peak pulse power of 8.57 mW by taking into account the repetition rate of the laser and Gaussian pulse shape. The optical spectrum is shown in Figure 6. The optical spectrum is centered at 1588.75 nm and has a 0.5 nm spectral width. This corresponds to a time bandwidth product of 0.42, indicating that the pulses are transform limited

5. Conclusions

Distributed feedback and an on chip mode locked laser have been demonstrated on the silicon evanescent device platform,

allowing for the integration of single wavelength and short pulsed laser sources with high performance silicon passive devices. The DFB-SEL lasing wavelength's dependence on silicon processing allows for precise wavelength control, and the ability to fabricate many DFBs perfectly matched with densely spaced multiplexors for low cost, high performance silicon transmitters. The racetrack ML-SEL enables integrated ODTM and single laser source WDM sources on a silicon platform.

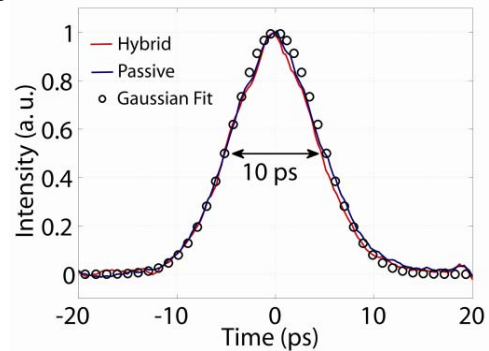


Figure 5: Autocorrelated pulse traces of the racetrack ML-SEL.

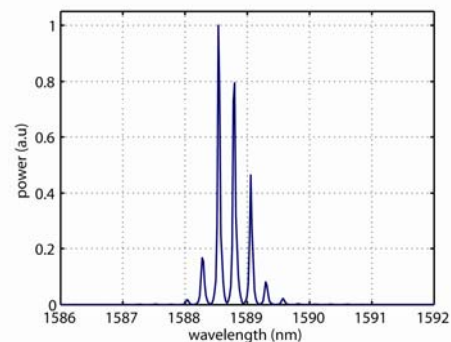


Figure 6: Optical spectrum of the racetrack ML-SEL.

Acknowledgements

This work was supported by a grant from Intel Corp. and from DARPA/MTO and ARL sponsored LASOR Project under the DODN program award number W911NF-05-1-0175 and W911NF-04-9-0001.

References

- [1] A. W. Fang, E. Lively, Y-H. Kuo, D. Liang, J. E. Bowers, *Optics Express*, 16, 4413-4419, 2008
- [2] A. W. Fang, B. R. Koch, K. Gan, H. Park, R. Jones, O. Cohen, M. J. Paniccia, D. Blumenthal, J. E. Bowers, *Optics Express*, 16, 1393-1398, 2008
- [3] A. W. Fang, H. Park, O. Cohen, R. Jones, M. J. Paniccia, and J. E. Bowers, *Optics Express*, 14, 9203-9210, 2006
- [4] Y.-H. Kuo, H.-W. Chen, J. E. Bowers, *OFC 2008*, San Diego, CA, 2008
- [5] H. Park, A. W. Fang, R. Jones, O. Cohen, O. Raday, M. N. Sysak, M. J. Paniccia, and J. E. Bowers, *Optics Express*, 15, 6044-6052, 2007